


Article

Energy Absorption and Damage Analysis of Fragments in High-Speed Impact on Composite Honeycomb Sandwich Structures

Bianhong Chang^{1,*}, Zhenning Wang¹ and Guangjian Bi² 

¹ College of Mechanical and Electrical Engineering, North University of China, Taiyuan 030051, China; wzn199603@163.com

² Chongqing Hongyu Precision Industry Group Co., Ltd., Chongqing 402760, China; bgjnuc@163.com

* Correspondence: changbianhong@nuc.edu.cn

Abstract: With the continuous innovation of UAV technology, composite honeycomb sandwich structures are used more and more in the fuselage structure of UAVs, and their anti-high-speed fragment impact performance has become a concern. In order to study the influence of fragments on the damage degree of composite honeycomb structures and analyze the damage difference of different initial velocity fragments on different composite honeycomb structures, based on the numerical simulation results of high-speed impact, the energy absorption characteristics of different honeycomb sandwich structures are analyzed, and the honeycomb structure with better energy absorption is selected for 24 impact experiments. The velocity range of fragment impact is 141–368 m/s. The typical damage of the upper core layer and the lower core layer in each structure is analyzed, and the energy absorption theory is used to compare the conditions of each group. The results show that ST-3-3 has the best energy absorption characteristics. Under different velocity impacts, the energy absorption per unit volume of the ST-3-3 structure reaches $521.6\text{--}659.6 \times 103 \text{ J/m}^3$, which is about 30.6% higher than that of the same design structure. The four groups of composite honeycomb sandwich structures designed in the experiment have obvious deformation in the process of impact, except that the deformation of the bottom skin of the ST-6-6-1 structure is not obvious, and the deformation of the other three groups is more obvious with the increase in structural resistance. This research shows that the reasonable arrangement of the structure and material of the composite honeycomb sandwich can better cope with the impact of high-speed fragments and reduce the damage to the structure.

Keywords: honeycomb sandwich; fragments; energy absorption characteristics; damage characteristics



Citation: Chang, B.; Wang, Z.; Bi, G. Energy Absorption and Damage Analysis of Fragments in High-Speed Impact on Composite Honeycomb Sandwich Structures. *Appl. Sci.* **2024**, *14*, 7303. <https://doi.org/10.3390/app14167303>

Academic Editor: Giangiacomo Minak

Received: 10 July 2024

Revised: 16 August 2024

Accepted: 18 August 2024

Published: 19 August 2024



Copyright: © 2024 by the authors. Licensee MDPI, Basel, Switzerland. This article is an open access article distributed under the terms and conditions of the Creative Commons Attribution (CC BY) license (<https://creativecommons.org/licenses/by/4.0/>).

1. Introduction

After experiencing the war in the Middle East, the war in Iraq, and the war in Asia, military drones have developed into two categories encompassing sixteen types [1–3]. With the continuous integration of cutting-edge scientific and technological achievements, military UAVs have greatly improved in terms of flight control, detection, stealth, penetration, and fire strike.

In recent years, this research on UAVs has made great progress in the direction of lightweight design. Nowadays, many structural parts of military UAVs, including parts, basically adopt lightweight honeycomb sandwich structures and composite materials. The ‘Predator’ UAV fuselage developed by General Atomics uses a large number of carbon fiber unidirectional prepregs and honeycomb sandwich structures. At the same time, carbon fiber beams and ribs are added to reduce the overall fuselage weight while ensuring strength. Its improved ‘Death’ uses the same fuselage structure but adds a new hybrid fiber prepreg. The ‘Shadow’ UAV produced by the AAI company uses a large number of reinforced epoxy resin structure skins and honeycomb sandwich structures, and the

total application amount exceeds 95% of the body structure. More than 90% of the body structure of the X-45 UAV developed by Boeing Company uses a low-temperature curing prepreg and foam sandwich structure [4–9].

At present, the weapons for typical targets in the air mainly include blast weapons, discrete rod warhead weapons, shaped charge warhead weapons, laser weapons, etc. The damage elements are mainly fragments, explosively formed projectiles, shaped charge jets, shaped charge rod penetrators, discrete rods, and other high-speed penetrators. Fragment penetration experiments are one of the main means to test the damage performance of composite structures and composites. Due to the different penetration speeds, it is generally divided into low speed, high speed, and ultra-high speed. The high-speed fragment penetration experiment is a common method for range testing. The initial velocity of the fragment is between 50 m/s–5000 m/s, which is used to analyze the flight attitude of the fragment, the power of the fragment, the failure mode, and the anti-elastic performance of the structure.

From this research on the composite honeycomb sandwich structure, the commonly used methods are static compression and low-speed collision. However, there are few studies on the energy absorption characteristics and damage modes of the structure under high-speed conditions. With the different application scenarios, the structural protection requirements are also different. In particular, it is necessary to analyze the damage characteristics of high-speed fragment penetration structures. The progress of theoretical analysis has promoted this research on honeycomb structure from the whole to the micro [10]. In the past, the commonly used theoretical analysis was to equivalentize the composite honeycomb sandwich structure into a laminated plate and then carry out the relevant theoretical damage calculation according to the characteristics of the laminated plate [11]. With the deepening of research, the honeycomb sandwich structure has gradually transitioned from the common equivalent analysis method to the level of quantitative analysis of the structure itself [12–16]. For honeycomb structures, the commonly used analysis methods are static compression, ballistic damage, and explosion shock. In the static compression state, the compressive strength is much smaller than the compressive strength under dynamic load. The plastic deformation area of the honeycomb structure is near the contact area between the sandwich structure and the penetrator, and its damage is mainly concentrated inside the specimen. During the penetration process, the structure is more likely to be destroyed, resulting in fiber breakage, debonding delamination, and even perforation. Zhang J.H. et al. [17] studied the nonlinear transient response of a honeycomb sandwich plate with a negative Poisson's ratio under an impact load, derived the partial differential equation of the honeycomb sandwich plate, and obtained the nonlinear ordinary differential equation of the structure by the truncation method. It was found that the negative Poisson's ratio honeycomb sandwich panel is better than the positive Poisson's ratio honeycomb sandwich panel. Similarly, Michele Baccocchi et al. [15] also used the higher-order shear theory to derive the partial differential equation for the critical buckling load of carbon nanotube-reinforced three-phase orthotropic honeycomb sandwich panels. Most of the remaining theoretical studies on honeycomb sandwich structures are basically developed based on the higher-order shear theory of laminates [11,14,16,18].

This research method of fragment penetration can be divided into two parts: high speed and ultra-high speed (greater than 5000 m/s), according to the speed. The analysis of sandwich structure in a high-speed state is common. The ballistic gun is the main launching source. The purpose is to analyze the failure mode, deformation mechanism, and protection performance of the honeycomb sandwich structure in a high-speed state. At present, the penetration of fragments into honeycomb sandwich structures at high speed is mainly based on numerical simulation. Buitrago B.L. et al. [19] used ABAQUS/Explicit to simulate the high-speed penetration of a honeycomb sandwich structure composed of carbon/epoxy resin skin and aluminum honeycomb core and determined the contribution of the failure mechanism of the honeycomb structure to the energy absorption of projectile kinetic energy. This study of the ultra-high-speed state is to use a two-stage hydrogen gun

to accelerate the bullet to more than 5000 m/s. High-speed photography technology and computer tomography technology are used to capture and observe the fragmentation of the projectile and the deformation and failure modes of the honeycomb sandwich structure, which provides a strong guarantee for the survivability of the spacecraft [20–22].

New materials, new structures, and new properties are the main research directions for honeycomb sandwich structures. In 2014, A. Gilioli et al. [23] conducted a penetration compression experiment on the sandwich structure composed of NOMEX™ core and aluminum plate and judged the relationship between penetration energy and residual strength. In 2018, Felipe de Souza Eloy et al. [24] designed a sandwich structure composed of carbon/epoxy composite skin and different proportions of magnetorheological elastomer core and carried out structural free vibration and forced vibration experiments under different magnetic field intensities to evaluate the dynamic performance of sandwich beams. In 2019, Jezrael Rossetti Dutra et al. [25] conducted a three-point bending test on the sandwich structure composed of an epoxy honeycomb core containing eucalyptus sawdust and cement particles and fiber palm fiber layer skin and analyzed the influence of structural parameters on core shear stress, surface stress, bending stiffness, and strength. In 2021, Du [26] tested the damage performance of the sandwich structure composed of glass fiber (GFRP) and carbon fiber (CFRP) hybrid skin and a NOMEX honeycomb core. It was found that the peak force was related to the penetration energy and the diameter of the punch. As the diameter of the punch increases, the peak force gradually increases.

Lv et al. [27] are still based on the NOMEX honeycomb core, but the skin is made of a multi-layer composite material that is bonded by a high-strength adhesive film. The penetration test of the structure was carried out using the drop hammer test machine. When the penetration energy is relatively low, the main energy dissipation of the structure is still dominated by the fiber tensile fracture of the composite skin. Zhang Y.W. et al. [28] compared the tube-reinforced honeycomb sandwich structure with the traditional honeycomb structure and found that the filling of the metal tube improved the stiffness and peak load of the traditional honeycomb structure, making the stress and deformation of the front and rear skins more uniform. The energy absorption characteristics of the structure are faster than those of the empty honeycomb structure, and the deformation of the front skin is reduced. In addition to the overall design of honeycomb structures, reports on this study of composite honeycomb structures have gradually increased. Yasui Y. et al. [29] conducted an experimental study on the impact and tensile properties of honeycombs with different matrix aluminum materials. It was found that the energy absorption effect of the pyramid-type tandem multi-layer honeycomb structure will be relatively improved after crushing. Li et al. [30] also carried out a numerical simulation and static compression test on the tandem aluminum honeycomb structure and obtained a buffer structure with better energy absorption characteristics.

It can be seen that the honeycomb sandwich structure of a new structure and new material is still one of the main research directions. The protection law and energy absorption characteristics of composite honeycomb sandwich structure in the face of other damage elements, especially for the related problems of composite honeycomb sandwich structure in high-speed collisions, need to be further studied. In this paper, in order to study the damage mode and anti-damage performance of composite honeycomb sandwich structure under high-speed fragment impact, four groups of composite honeycomb sandwich structure and two groups of comparative structure were studied by fragment impact experiment. The damage law of the composite honeycomb sandwich structure under different velocities of fragment was analyzed, and the energy absorption characteristics of the composite honeycomb sandwich structure under fragment impact were compared and analyzed according to the experimental results.

2. Numerical Simulation Analysis of Fragment Impact Composite Honeycomb Sandwich Structure

2.1. Modeling and Materials

In this paper, Truegrid 3.1.3 is used for modeling. The honeycomb structure adopts the Lagrange grid, which is a hexahedral entity element with 8 nodes. In order to ensure calculation accuracy, the grid density of the honeycomb structure in the impact zone is larger. The time step of the calculation is reduced, thus increasing the number of iterations. Because the composite model is symmetrical, in order to reduce the number of calculation units, a quarter model is established for calculation. Due to the different structural sizes, the cell size is small with about 300,000 grids, and the cell size is large with about 210,000 grids. In order to change the variables of the honeycomb sandwich structure, the numerical simulation model of the composite honeycomb sandwich structure with adjustable structural parameters is obtained by using the parametric modeling method. The core layer and the overall modeling process are shown in Figure 1.

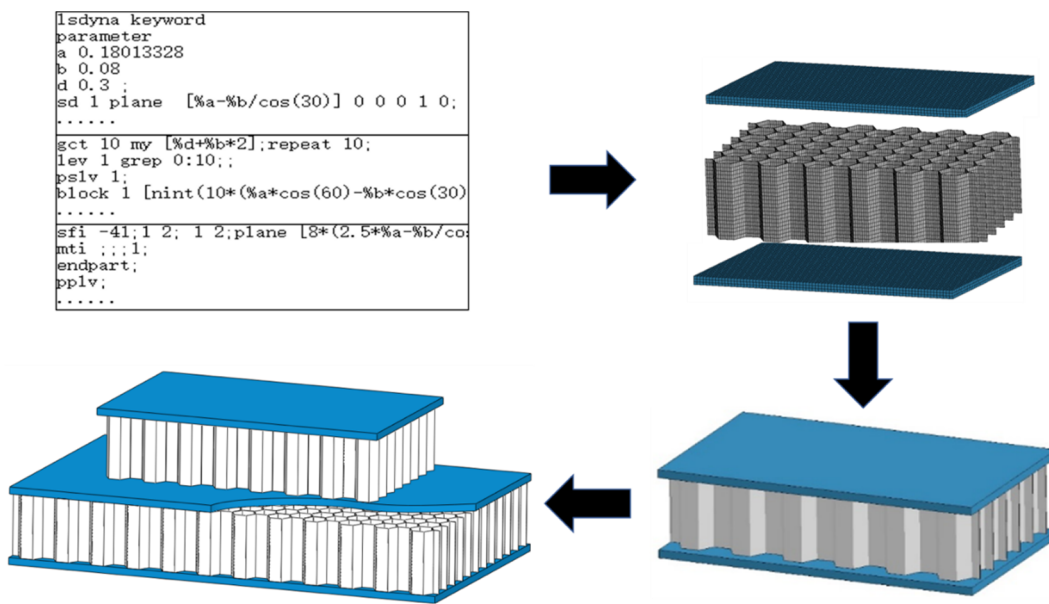


Figure 1. Modeling process of composite honeycomb sandwich structure.

The high-speed fragment model is designed with a cylindrical structure with a diameter of 12 mm and a height of 30 mm. The speed is set to 200 m/s. The material is 45# steel. In the simulation process, in order to eliminate the influence of fragment deformation on structural damage characteristics, the finite element model of the fragment is set as a rigid body.

In this study, the solver used ANSYS LS-DYNA18.2. The composite honeycomb sandwich structures designed in this paper all use Lagrange algorithm. The material models are MAT_JOHNSON_COOK model and EOS_GRUNEISEN state equation.

The flow stress of the material is expressed as the product of strain function, strain rate function, and temperature function, which can reflect the influence of strain strengthening, strain rate strengthening effect, and temperature softening effect of the material. The expression is:

$$\rho = (A + B\varepsilon^m) \left(1 + C \ln \dot{\varepsilon}^*\right) (1 - T^{*n}) \tag{1}$$

Here σ is the plastic flow stress of the material; ε^p is the equivalent plastic strain; $\dot{\varepsilon}^*$ is the relative equivalent plastic strain rate; T^* is the dimensionless temperature term; A is the initial yield stress at reference temperature and reference strain rate, B is the strain hardening modulus of the material, C is the strain rate sensitivity coefficient, n is the

hardening index of the material, and m is the temperature softening coefficient. T_m is the melting temperature; T_r is the room temperature.

The flow stress of the material is expressed as the product of strain function, strain rate function, and temperature function, which can reflect the influence of strain strengthening, strain rate strengthening effect, and temperature softening effect of the material. The honeycomb core material in the composite honeycomb sandwich structure is 2024 Aluminum and 304 stainless steel, and the skin material is a 7075 Aluminum alloy. The specific parameters of the material model are shown in Table 1.

Table 1. Material parameter.

Material	ρ (kg/m ³)	G (GPa)	A (GPa)	B (GPa)	n	c	m	T_m (K)	T_r (K)
7075 Aluminum	2810	26.9	0.520	0.477	0.52	0.0025	1.61	893	293
2024 Aluminum	2780	28.6	0.265	0.426	0.34	0.015	1	775	300
Stainless steel	7890	77	0.278	1.3	0.8	0.072	0.81	1800	298

MAT_PLASTIC_KINEMATIC was selected for the two groups of structural models. The material density of NOMEX was 144 Kg/m³, the Young’s modulus was 1.13, the Poisson’s ratio was 0.38, the yield stress of the material was 3.34×10^{-5} , and the failure strain of the material was 0.8. The material density of FIBER is 1740 Kg/m³, the Young’s modulus is 2.30, the Poisson’s ratio is 0.307, the yield stress of the material is 9×10^{-5} , and the failure strain of the material is 0.9.

The contact between the skin and the core is a fixed connection failure method. The contact surface between the skin and the core is firmly connected, allowing the two surfaces to slide and separate from each other after failure. The deformation of the honeycomb core is a complex process. In addition to the contact between the skin and the core, the honeycomb cells themselves also interact. Therefore, the honeycomb core is automatically set to face-to-face contact. The honeycomb structure adopts the Lagrange grid, which is a hexahedral solid element with 8 nodes. At the same time, the preprocessing problem of the finite element model is established by K file. In order to ensure calculation accuracy, the grid density of the honeycomb structure in the impact zone is large. The time step of the calculation is reduced, thus increasing the number of iterations. The displacement of the edge of the composite honeycomb structure is prevented, so the degree of freedom of the solid elements at the edge in the X, Y, and Z directions is limited. The rest of the solid elements have six degrees of freedom for the displacement and rotation of X, Y, and Z. At the same time, the operation k file of the model is written to reduce the TSSFAC keyword in CONTROL_TIMESTEP and shorten the time step to improve the accuracy of the operation results.

In order to analyze the influence of cell composite mode on the damage resistance of honeycomb sandwich structures, a total of 18 groups of structures were designed for numerical simulation of high-speed fragment impact. Among them, the skin material in 1#–17# is 7075 Aluminum, and 18# is unidirectional carbon fiber, as shown in Table 2.

Table 2. Material and structure size match.

NO.	Upper Parameters		Lower Parameters		NO.	Upper Parameters		Lower Parameters	
	Material	Diameter	Material	Diameter		Material	Diameter	Material	Diameter
1#	Al	d3	Al	d3	10#	St	d3	St	d6.4
2#	Al	d3	Al	d6.4	11#	St	d6.4	St	d3
3#	Al	d6.4	Al	d3	12#	St	d6.4	St	d6.4
4#	Al	d6.4	Al	d6.4	13#	St	d3	Al	d3
5#	Al	d3	St	d3	14#	St	d3	Al	d6.4
6#	Al	d3	St	d6.4	15#	St	d6.4	Al	d3
7#	Al	d6.4	St	d3	16#	St	d6.4	Al	d6.4
8#	Al	d6.4	St	d6.4	17#	NOMEX	d3	Al	d3
9#	St	d3	St	d3	18#	NOMEX	d3	C	d3

2.2. Numerical Simulation Results Analysis

The overall damage and core damage effects of the 1#–16# structure in the numerical simulation are shown in Figure 2.

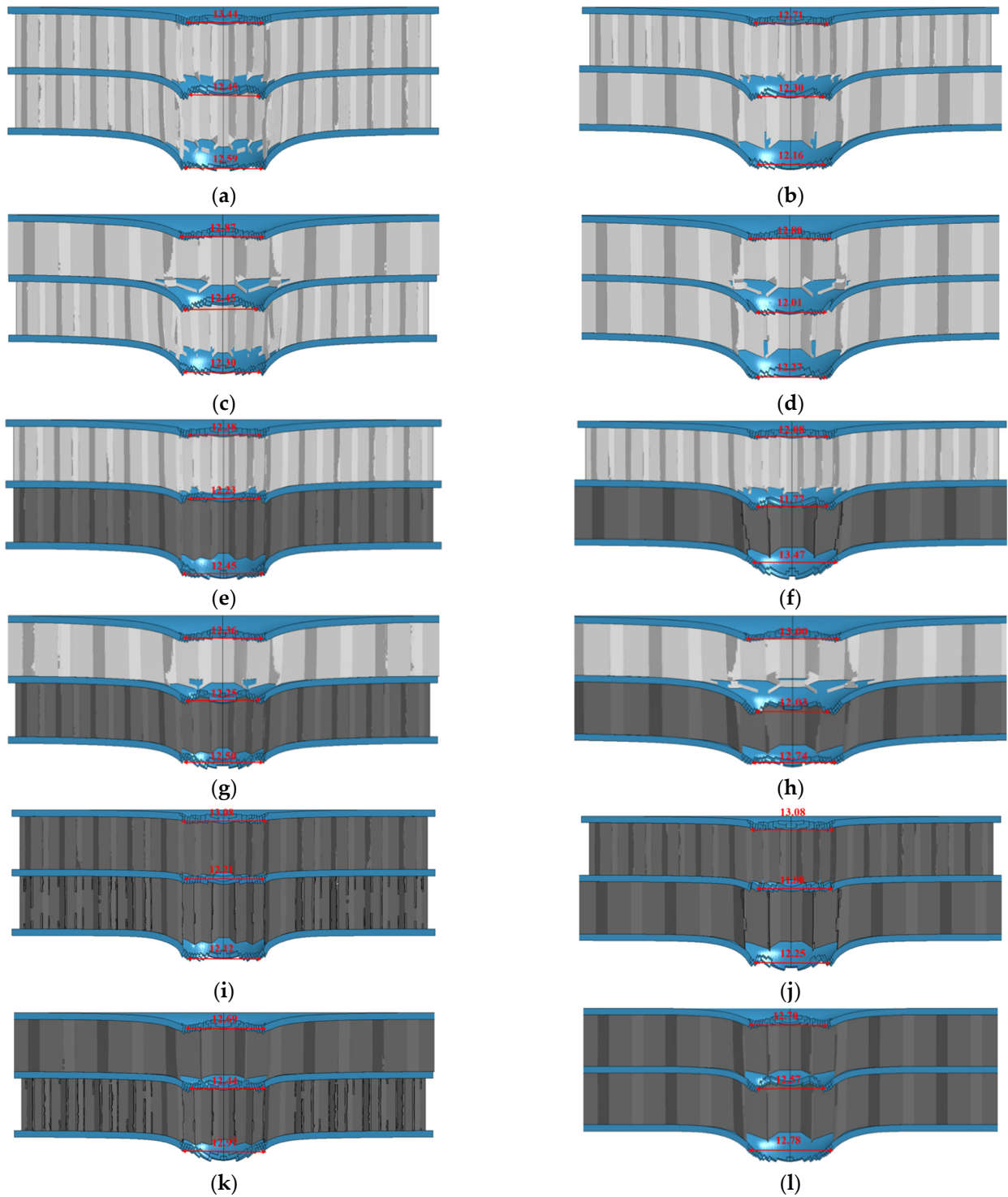


Figure 2. Cont.

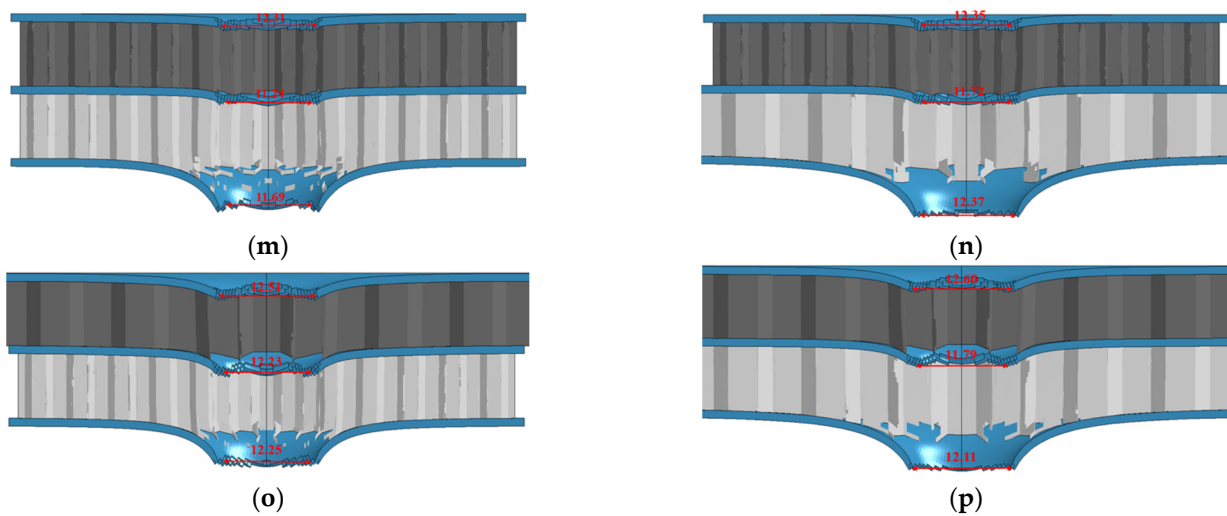


Figure 2. Damage to 16 groups of honeycomb structures. (a–p) are separately for 1#–16#.

For these two composite methods, the minimum opening diameter of the skin is concentrated in the middle skin position, where the strength of the lower material is high, which indicates that the strength of the lower core material has a great influence on the opening diameter of the middle skin. The higher the strength, the greater the bearing capacity of the middle skin; the deformation to the impact direction of the fragment is completely limited; and the shear effect around the fragment increases, resulting in the minimum opening of the structure. The position of the middle skin is at the middle skin position, and the opening is relatively neat, and the tensile strength of the material is not obvious. Based on the overall damage to all structures and the damage to the core layer, the influence of the 16 composite methods designed on the degree of structural deformation is different. Among them, the overall deformation of the small-sized high-strength material composite structure is small, and the impact resistance is relatively high. The second is the honeycomb sandwich structure composed of two different strength materials, and the structure composed of low-strength and high-plastic materials has a relatively poor effect. For a structure with the same average cell density and different combinations of upper and lower core materials, the damage situation is not much different, but it has a certain influence on the deformation degree of the overall structure. The lower the strength of the lower layer material, the greater the overall deformation of the structure. On the contrary, with the increase in strength of the lower core layer, the deformation of the overall structure is relatively small. It can be seen that the anti-damage performance of the composite honeycomb sandwich structure is determined by the composite method, material selection, and core size ratio.

According to the law of conservation of energy, the total energy absorption of the structure in each case is obtained, as shown in Table 3.

Due to the different composition of the structure, a simple analysis of the overall energy absorption of the composite honeycomb sandwich structure cannot reflect the real energy absorption characteristics of the structure. Therefore, this paper measures the energy absorption effect of the structure by the energy absorption index per unit volume, that is:

$$EPV = \frac{EAT}{V} \quad (2)$$

EAT is the total energy absorption of the structure, and EPV is the energy absorbed by the unit volume of the structure. Table 4 shows the numerical simulation results of energy absorption per unit volume for 18 types.

Table 3. Residual velocity and energy absorption rate of fragments (Numerical simulation data).

NO.	Remaining Velocity v_r (m/s)	Total Energy Absorption J	NO.	Remaining Velocity v_r (m/s)	Total Energy Absorption J
1#	157.5	204.35	10#	152	227.25
2#	158.4	200.53	11#	151	231.32
3#	159.3	196.68	12#	155	214.86
4#	160	193.68	13#	154	219.01
5#	151	231.32	14#	153	223.14
6#	159	197.97	15#	157	206.47
7#	150.6	232.95	16#	157.4	204.78
8#	155	214.86	17#	175	126.09
9#	145	255.21	18#	191	47.33

Table 4. Energy absorption per unit volume of 18 types (Numerical simulation data).

NO.	Energy Absorption per Unit Volume ($\times 10^3$ J/m ³)	NO.	Energy Absorption per Unit Volume ($\times 10^3$ J/m ³)
1#	478	10#	531
2#	469.1	11#	541.1
3#	460.1	12#	502.6
4#	451.4	13#	512.3
5#	541.1	14#	521.9
6#	463	15#	482.9
7#	544.9	16#	479
8#	502.6	17#	294.9
9#	596.5	18#	110.7

From the energy absorption per unit volume, it can be seen that the energy absorption effect of the designed 16 groups of composite honeycomb sandwich structures is much larger than that of the two groups of structures. The minimum energy absorption per unit volume is 53% and 307% higher than that of NOMEX-AL and NOMEX-C structures, and the maximum value is 102.3% and 438.8% higher, respectively.

Combined with the overall failure mode of 16 groups of structures, the core failure mode, and the energy absorption per unit volume, it can be found that among all the composite methods, the structure with the best energy absorption effect and the best impact resistance and deformation ability is the 9# structure with the upper and lower core cell diameters of 3 mm, and the energy absorption per unit volume is 596.5 J/m³.

3. Experimental Design of Fragment-Penetrating Composite Honeycomb Sandwich Structure

3.1. Type of Structure of the Specimen

Four groups of composite honeycomb sandwich structures and two groups of contrast structures were subjected to high-speed fragment impact experiments. The experimental specimens are shown in Figure 3.

Among them: AL/NOMEX indicates that NOMEX is a honeycomb core, and the skin is 7075 Aluminum; c/NOMEX indicates that NOMEX is a honeycomb core and carbon fiber is skin; the Figure 3e,f structure is 304 stainless steel honeycomb core, and the skin material is 7075 Aluminum. Top represents the upper honeycomb structure; Bottom represents the lower honeycomb structure; D = 3 mm indicates that the core cell diameter is 3 mm; and D = 6.4 mm indicates that the core cell diameter is 6.4 mm.

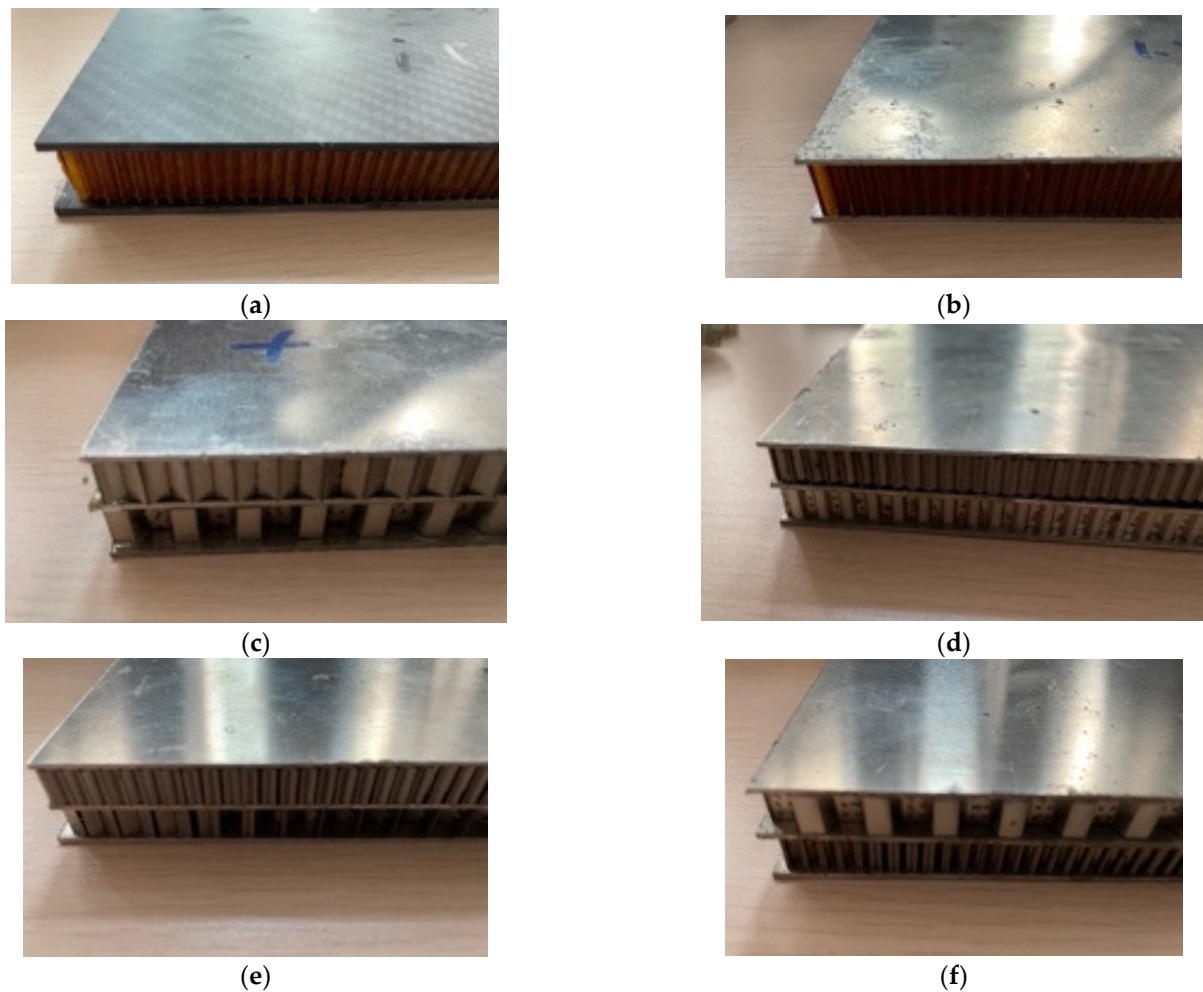


Figure 3. Honeycomb sandwich structure specimen. (a) is C/NOMEX; (b) is Al/NOMEX; (c) is Top D = 6.4 mm/Bottom D = 6.4 mm; (d) is Top D = 3 mm/Bottom D = 3 mm; (e) is D = 3 mm/Bottom D = 6.4 mm; (f) is Top D = 6.4 mm/Bottom D = 3 mm.

3.2. Test Scheme

Six types of structures were subjected to high-speed fragment penetration experiments. The fragment weighs 26.9 g, with a diameter of 12 mm and a length of 30 mm. In the experiment, 150 mm × 150 mm and 300 mm × 300 mm composite honeycomb sandwich structures were subjected to high-speed fragment penetration. The size of the fixture is 276 mm × 276 mm and 400 mm × 400 mm, in which the reserved penetration area of the small size fixture is 90 mm × 90 mm and the penetration area of the large size fixture is 220 mm × 220 mm. In order to meet the size requirements of the fixed steel frame at the experimental site, the small fixture can be embedded in the large fixture, and the surrounding frame is filled with square wood. The experimental fixture of the composite honeycomb sandwich structure is shown in Figure 4.

The small specimen fixture is fastened by six bolts with a diameter of 20 mm, and the large specimen fixture is fastened by nine bolts with a diameter of 30 mm. The assembled target plate is fixed by four U-shaped clamps on a 500 mm × 500 mm steel frame with a stable seat. The fragments and the shell are connected by the elastic support and pressed by the press. The total length of the fragments and the shell is 160 mm. The fragments are cylindrical, 12 mm in diameter, and 30 mm in height. The same projectile parameters as in the experiment are used in the numerical simulation. The experimental propellant uses black gunpowder + camphor gunpowder. The amount of black gunpowder is 1 g, and the amount of camphor gunpowder is controlled to ensure a change in the initial velocity

of the fragment. In the experiment, a high-speed camera was used to record the whole process of fragment emission, impact on the target plate, and flight after penetration. The first benchmark was set up at 452 mm in front of the target, and the second benchmark was set up at 590 mm behind the target. In the field of high-speed photography, the target plate and two benchmarks are included. The initial impact velocity of the fragment (the velocity before hitting the target plate) and the residual velocity (the velocity after penetrating the target plate) are calculated by observing the distance of the fragment movement in the video, the recording time of the high-speed photography, and the markers. The experimental site layout is shown in Figure 5.

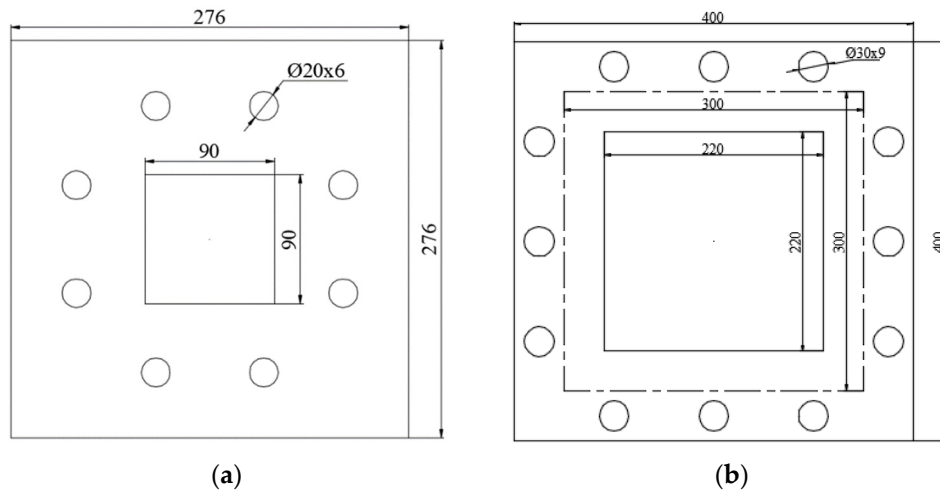


Figure 4. Specimen clamp. (a) is 150 mm × 150 mm; (b) is 300 mm × 300 mm.

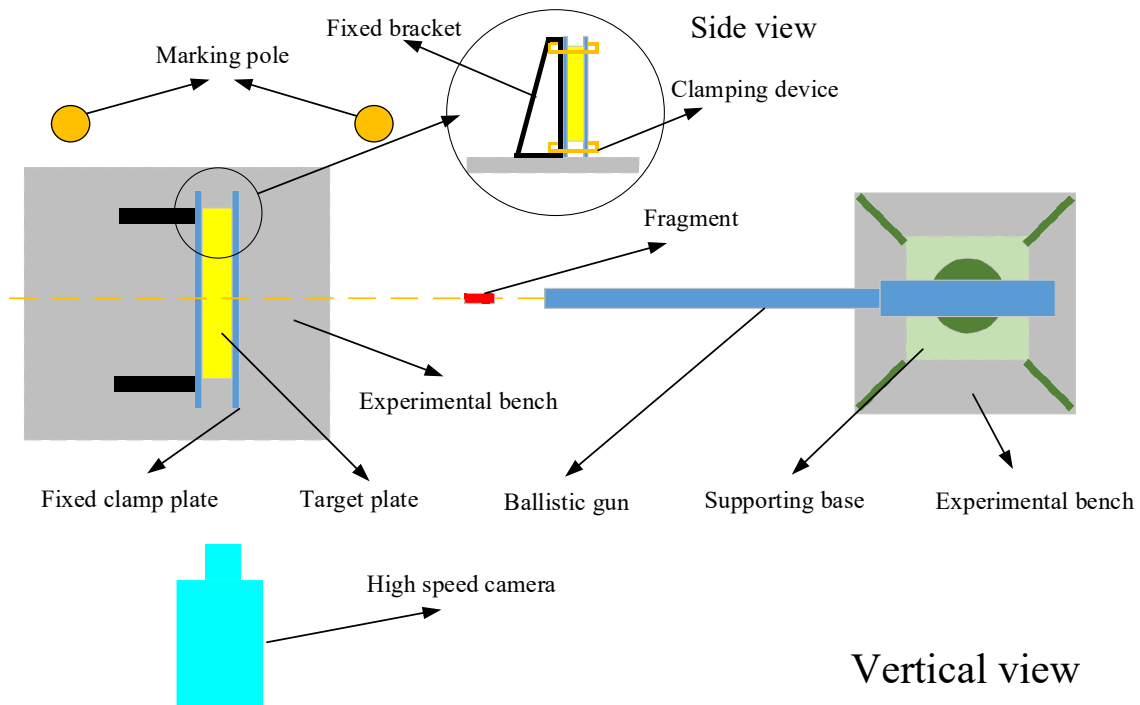


Figure 5. Layout of test site.

In this experiment, the anti-damage characteristics of six honeycomb sandwich structures at different penetration speeds were studied. The experimental scheme and the collected data are shown in Table 5.

Table 5. Test plan (Experimental data).

NO.	Type	Numbering/#	Initial Velocity v_r (m/s)	Remaining Velocity v_i (m/s)
1	NOMEX-AL-1	1#	188.3	173.5
2		2#	226	210.7
3		3#	265.8	256.5
4		4#	368.4	348.4
5	NOMEX-C-1	1#	141.3	131.1
6		2#	226	218.5
7		3#	265.9	256.5
8		4#	301.3	295
9	ST-6-6-1	1#	161.4	118
10		2#	226	196.7
11		3#	265.9	236
12		4#	322.9	295
13	ST-6-3-1	1#	150.7	75.6
14		2#	196.5	178.8
15		3#	265.9	245.9
16		4#	322.9	295
17	ST-3-6-1	1#	161.4	98.3
18		2#	226	190.3
19		3#	265.9	245.8
20		4#	322.9	281
21	ST-3-3-1	1#	150.7	67.8
22		2#	226	173.5
23		3#	237.9	190.3
24		4#	307.3	279

Among them, NOMEX-AL-1 indicates that NOMEX is a honeycomb core and the skin is a 1# target plate of 7075 Aluminum; NOMEX-C-1 indicates that NOMEX is a honeycomb core and carbon fiber is a 1# target plate of the skin. ST-3-3-1 indicates that 304 stainless steel is a 1# target plate with a honeycomb core and a cell diameter of 3 mm in the upper and lower core layers. ST-3-6-1 indicates that 304 stainless steel is a honeycomb core, and the 1# target plate with the upper core cell diameter of 3 mm and the lower core cell diameter of 6.4 mm; sT-6-3-1 indicates that 304 stainless steel is a honeycomb core, and the 1# target plate with a core cell diameter of 6.4 mm and a core cell diameter of 3 mm; sT-6-6-1 indicates that 304 stainless steel is a honeycomb core, and the cell diameter of the upper and lower core layers is 1# target plate of 6.4 mm.

It can be seen from Table 6 that when the speed is less than 400 m/s, with the increase in speed, the theoretical results, numerical simulation results, and experimental results are not much different, and the curves of each group have the same trend of change, basically rising linearly. There is little difference between the numerical simulation results and the experimental results. It can be seen that the numerical simulation modeling method of the fragment-penetrating composite honeycomb sandwich structure proposed in this paper is in line with engineering practice, and the error is relatively small. Excluding other influencing factors, the average error between the numerical simulation value and the experimental result is 4.10%.

Table 6. Residual velocity of test and simulation (Calculated data).

NO.	Type	Initial Velocity (m/s)	Numerical Simulation of Residual Velocity (m/s)	Experimental Results Residual Velocity (m/s)	Numerical Simulation and Experimental Error
1	NOMEX-AL-1	188.3	179	173.5	3.17%
2		226	211	210.7	0.14%
3		265.8	252	256.5	1.75%
4		368.4	353	348.4	1.32%
5	NOMEX-C-1	141.3	135	131.1	2.97%
6		226	216	218.5	1.14%
7		265.9	255	256.5	0.58%
8		301.3	289	295	2.03%
9	ST-6-6-1	161.4	124.1	118	5.17%
10		226	196.3	196.7	0.20%
11		265.9	241.1	236	2.12%
12		322.9	302.8	295	2.64%
13	ST-6-3-1	150.7	89.5	75.6	18.39%
14		196.5	154.6	178.8	13.5%
15		265.9	231	245.9	6.05%
16		322.9	294.8	295	0.07%
17	ST-3-6-1	161.4	106.5	98.3	8.34%
18		226	183.6	190.3	3.52%
19		265.9	231	245.8	6.02%
20		322.9	294.8	281	4.91%
21	ST-3-3-1	150.7	62	67.8	8.55%
22		226	170.1	173.5	1.96%
23		237.9	190.3	190.3	0%
24		307.3	268	279	3.94%

3.3. Analysis of Test Results

A total of 24 penetration experiments were carried out on six honeycomb structures, and the damage to each structure at different penetration speeds was obtained. The minimum penetration velocity is 141.3 m/s, and the maximum penetration velocity is 368.4 m/s. The damage to each structure at four speeds of 140 m/s–380 m/s is shown in Figure 6. The ‘+’ represents the front of the honeycomb sandwich panel, and the ‘−’ represents the back of the honeycomb sandwich panel.

Each structure is divided into 1#–4# according to the impact order. It can be seen from Figure 5 that the NOMEX-AL structure has regular holes and no obvious deformation under high-speed impact. The pore size of the carbon fiber front skin is almost the same as that of the fragment under shear action, and the back skin has a tendency to return to the original state after the fragment is broken down due to the performance of the material itself. The opening diameter of the front skin is similar to the diameter of the fragment, and the diameter of the rear skin is different. The carbon fiber skin is covered by the damaged material with a small aperture. By comparing the two different types of skin materials, NOMEX-AL and NOMEX-C, it can be seen that the back skin of the AL material deforms more during the impact process, while the skin of the C material deforms less, which will

cause the honeycomb sandwich connected to the skin material to absorb more energy and cause greater collateral damage.

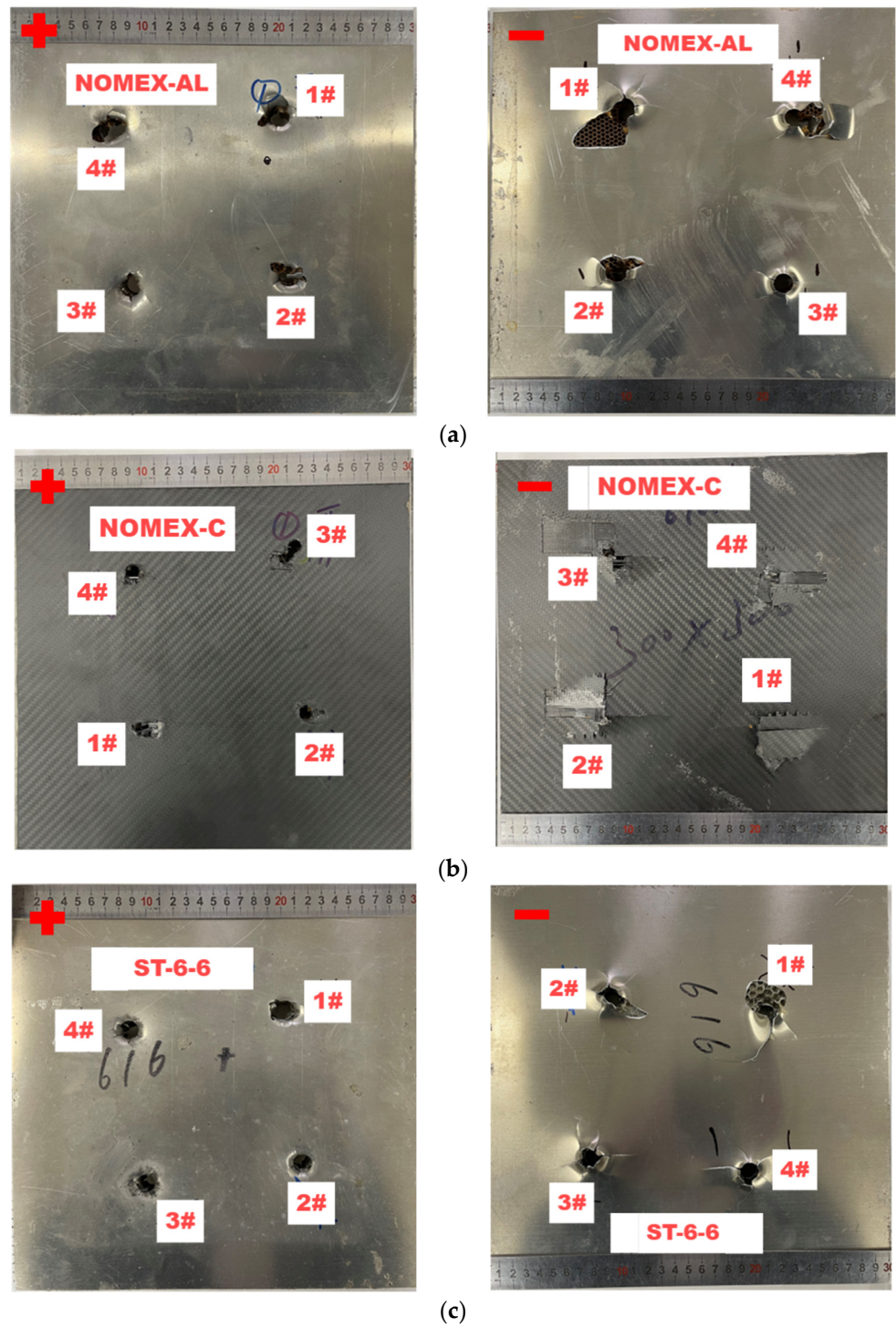


Figure 6. Cont.

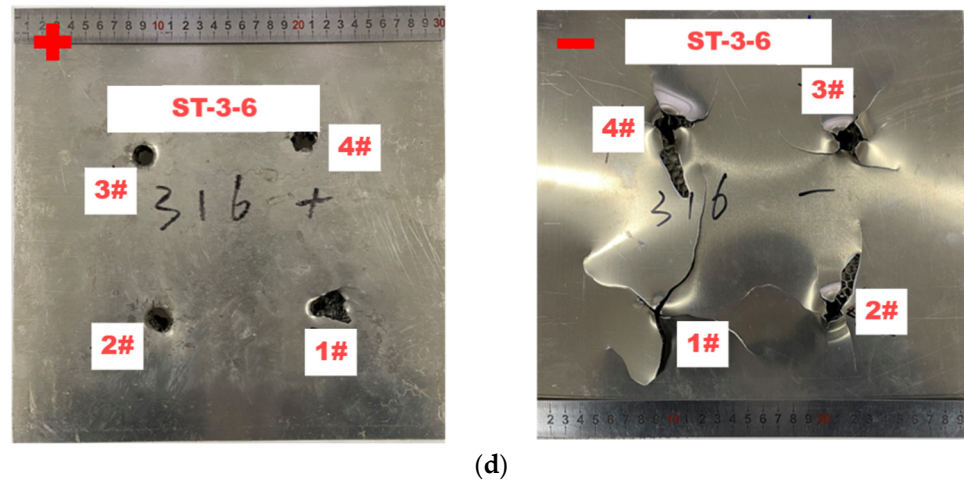


Figure 6. Damage to six structures at different velocities. (a) is NOMEX-AL-1; (b) is NOMEX-C-1; (c) is ST-6-6-1; (d) is ST-3-6-1.

Compared with the composite honeycomb sandwich structure of four ST materials, it can be seen that the opening shape of the impact front of the target plate is more regular, but the impact resistance of the two groups with the upper honeycomb diameter of 3 mm is better than that of the two groups with the honeycomb diameter of 6.4 mm because the depression range of the front of the target plate is smaller and there is almost no depression in the same speed range. At the same time, damage to the back target plate is also more likely to occur when the diameter of the lower honeycomb is small. Due to the stronger connection ability of the 3 mm honeycomb diameter, the joint damage on the back of the target plate is greater.

The four groups of composite honeycomb sandwich structures designed by have obvious deformation in the process of impact except for the bottom skin deformation of the ST-6-6-1 structure, and the deformation is more obvious with the increase in structural resistance. From the point of view of damage, when the honeycomb diameter of the lower honeycomb structure is larger, the incidental damage to the whole structure is smaller.

3.4. Analysis of Energy Absorption Characteristics of Composite Honeycomb Sandwich Structure

In addition to the direct observation of the damage to the structure, the energy absorption characteristics of the honeycomb sandwich structure are also the main indicators used to measure the damage performance of the structure. The total energy absorption and structural energy absorption rates are commonly used mathematical research methods.

In the state of high-speed penetration, the total energy absorption of the structure is obtained by using the law of conservation of energy according to the different velocities after penetrating the target. Assuming that the energy dissipation in the process of fragment penetration is absorbed by the sandwich structure, then

$$W_{TE} = W_R + W_E \tag{3}$$

W_{TE} is the total energy, that is, the initial kinetic energy of the fragment; W_R is the residual kinetic energy of the fragment; and W_E is the total energy absorbed by the sandwich structure.

$$W_{TE} = 0.5mv_r^2 \tag{4}$$

$$W_R = 0.5mv_i^2 \tag{5}$$

where m is the mass of the fragment, v_r is the residual velocity of the fragment, and v_i is the initial velocity of the high fragment. Then, the total energy absorption of the sandwich structure is:

$$W_E = W_{TE} - W_R = 0.5m(v_i^2 - v_r^2) \tag{6}$$

The initial velocity v_i and the residual velocity v_r are given in Table 5.

Combined with the energy absorption index per unit volume, the 24 sets of data from the experiment were sorted out to obtain the total energy absorption and energy absorption per unit volume of all structures. The specific results are shown in Table 7.

Table 7. Energy absorption of composite honeycomb sandwich structure (Calculated data).

NO.	Total Energy Absorption (N/m)	Energy Absorption per Unit Volume ($\times 10^3$ J/m ³)	NO.	Total Energy Absorption (N/m)	Energy Absorption per Unit Volume ($\times 10^3$ J/m ³)
1#	72	168.4	13#	229	535
2#	89.9	210.3	14#	89.3	208.9
3#	65.3	152.7	15#	138	322.8
4#	193	451.5	16#	232	542.7
5#	37.4	87.5	17#	220	514.6
6#	44.8	104.8	18#	200	467.8
7#	66	154.4	19#	138	322.8
8#	50.5	118.1	20#	340	795.3
9#	163	381.3	21#	244	570.8
10#	167	390.6	22#	282	659.6
11#	202	472.5	23#	274	641
12#	232	542.7	24#	223	521.6

It can be seen from Table 7 that, in addition to the influence of field factors on the deflection of fragments, with the increase in fragment impact velocity, the total energy absorption per unit volume of six kinds of sandwich structures is also increasing gradually. Comparing the two skin materials, AL and C, it can be seen that the overall dynamic response of the metal material to the honeycomb sandwich structure is more obvious, so that the energy absorption value of the structure is larger.

The range of the three structures of ST-6-6, ST-6-3, and ST-3-6 reaching the peak is mainly concentrated in the impact velocity of more than 200 m/s. With the increase in fragment impact velocity, the overall energy absorption of each honeycomb structure basically shows an upward trend, and the overall energy absorption of ST-3-3 is the largest. The average cell density of ST-6-3 and ST-3-6 is the same, and the total energy absorption under different impact velocities is not much different from the energy absorption per unit volume. However, with the increase in impact velocity, the energy absorption trend of the two structures is not as obvious as that of ST-6-6.

4. Conclusions

The composite honeycomb sandwich structure is more and more applied to the field of UAV, and the impact resistance of the honeycomb structure is becoming more and more important. The performance of the composite honeycomb structure under impact is compared by numerical simulation, and its damage characteristics and the residual velocity of the fragment are analyzed. Four structures with better energy absorption characteristics are obtained by using the energy absorption criterion. In order to verify the accuracy of the theoretical model and the calculation method of fragment residual, the damage performance of the composite honeycomb sandwich structure impacted by fragments at different speeds was experimentally studied. The actual damage characteristics of the honeycomb sandwich structure were analyzed. Based on the energy absorption characteristics of the structure, the response differences of different structures to impact energy were obtained. The main conclusions are as follows:

(1) The upper and lower core layers are all stainless steel. The structure with a cell diameter of 3 mm has the strongest impact resistance, and the energy absorption is about 30.6% higher than the other three design structures, which is consistent with the experimental test and numerical simulation results. In the test speed range, the unit volume energy absorption of the optimized composite honeycomb sandwich structure reaches 521.6×10^3 J/m³– 659.6×10^3 J/m³.

(2) The damage diameter of the front skin of the composite honeycomb sandwich structure is similar to the diameter of the fragment, and the damage diameter of the rear skin is different. The carbon fiber skin is blocked by the damaged material. The aperture is small, and the mechanical response of the whole structure is more obvious when the skin material is metal. The different degrees of damage to the rear skin of the composite honeycomb sandwich structure are mainly affected by the skin material and the honeycomb diameter. When the honeycomb diameter is 3 mm, the connection effect on the rear skin is more obvious, resulting in increased collateral damage at the rear.

(3) The four groups of composite honeycomb sandwich structures designed have obvious deformation in the process of impact, except that the deformation of the bottom skin of the ST-6-6 structure is not obvious, and the deformation is more obvious with the increase in structural resistance. The velocity load characteristics of the composite honeycomb sandwich structure are obvious, and the residual velocity curve of the fragment after the low-speed impact structure can show a linear trend.

Through the numerical simulation and experimental test of the four composite honeycomb sandwich structures, it is shown that the material model and simulation method used in the numerical simulation have certain engineering significance and can be used to test the energy absorption effect of the structure in the high-speed range. It can be seen from the comprehensive analysis of the damage results and the overall energy absorption of the honeycomb sandwich structure that a reasonable structural design scheme is needed to reduce the overall damage, and the sandwich structure can greatly improve the total energy absorption, thereby reducing the damage to other parts and improving the protection performance of the system.

Author Contributions: Conceptualization, B.C. and G.B.; Methodology, B.C.; Software, G.B.; Validation, B.C.; Investigation, B.C. and Z.W.; Experiment, G.B.; Data curation, G.B.; Writing—original draft preparation, B.C.; Writing—review and editing, G.B. and Z.W.; Supervision, G.B.; Project administration, G.B. All authors have read and agreed to the published version of the manuscript.

Funding: The authors would like to acknowledge the financial support from the project supported by the Fund Project of the North University of China Postgraduate Science and Technology Project (grant number: 20231904).

Institutional Review Board Statement: Not applicable.

Informed Consent Statement: Not applicable.

Data Availability Statement: The data presented in this study are available on request from the corresponding author. The data are not publicly available due to programming privacy in the structural design.

Conflicts of Interest: Author Guangjian Bi was employed by the company Chongqing Hongyu Precision Industry Group Co., Ltd. The remaining authors declare that the research was conducted in the absence of any commercial or financial relationships that could be construed as a potential conflict of interest.

References

1. Qing, X.C.; Liu, X.D.; Chen, D.L. Research on the Characteristics of Military Drone Use. *Heilongjiang Sci. Technol. Inf.* **2008**, *36*, 11.
2. Chen, L.; Chang, L. Analysis of the Development of Demon Unmanned Verification Aircraft and Jet Flight Control Technology in the UK. *Aerodyn. Missile J.* **2011**, *10*, 56–59.
3. Yang, X.B. The Incubator of Future Technology—UK “Devil” Drones. *Small Arms* **2011**, *12*, 23–25.
4. Ni, N.N.; Bian, K.; Xia, L.; Gu, W.K.; Wen, Y.F. Application of advanced composite materials for UAV. *J. Aeronaut. Mater.* **2019**, *39*, 45–60.
5. Shen, L.; Ou, Y.P. Characteristics and Development Experience of Predator Series Drones. *Aerodyn. Missile J.* **2012**, *12*, 33–36.
6. Liu, Y.; Li, Y.B.; Wang, Y.Y. Predator Shows Features of HALE Reconnaissance And Strike UAV. *Int. Aviat.* **2009**, *12*, 26–28.
7. Yu, F. Predator C, Avenger Made First Test Flights. *Int. Aviat.* **2009**, *6*, 28–30.
8. Cheng, D.L. Structure and Function of Composite Material and Its Application in Unmanned Aerial Vehicle Field. *Contemp. Chem. Ind.* **2019**, *1*, 125–127.
9. Yuan, L.Q.; Shan, H.Y.; Yang, Z.Q. The Application and Prospect of Composite Materials in UAV. *Fiberglass J.* **2017**, *6*, 30–36.

10. Greco, F. A study of stability and bifurcation in micro-cracked periodic elastic composites including self-contact. *Int. J. Solids Struct.* **2013**, *50*, 1646–1663. [[CrossRef](#)]
11. Levinson, M. An accurate, simple theory of the statics and dynamics of elastic plates. *Mech. Res. Commun.* **1980**, *7*, 343–350. [[CrossRef](#)]
12. Nayak, S.K.; Singh, A.K.; Belegundu, A.D. Process for design optimization of honeycomb core sandwich panels for blast load mitigation. *Struct. Multidiscip. Optim.* **2013**, *47*, 749–763. [[CrossRef](#)]
13. Hu, L.L.; You, F.F.; Yu, T.X. Analyses on the dynamic strength of honeycombs under the y-directional crushing. *Mater. Des.* **2014**, *53*, 293–301. [[CrossRef](#)]
14. Whitney, J.M.; Pagano, N.J. Shear Deformation in Heterogeneous Anisotropic Plates. *J. Appl. Mech.* **1970**, *37*, 1031–1036. [[CrossRef](#)]
15. Baccocchi, M.; Tarantino, A.M. Critical buckling load of honeycomb sandwich panels reinforced by three-phase orthotropic skins enhanced by carbon nanotubes. *Compos. Struct.* **2020**, *237*, 111904. [[CrossRef](#)]
16. Whitney, J.M.; Sun, C.T. A higher order theory for extensional motion of laminated composites. *J. Sound Vib.* **1973**, *30*, 85–97. [[CrossRef](#)]
17. Zhang, J.; Zhu, X.; Yang, X. Transient Nonlinear Responses of an Auxetic Honeycomb Sandwich Plate under Impact Loads. *Int. J. Impact Eng.* **2019**, *134*, 103383. [[CrossRef](#)]
18. Reddy, J.N. A Simple Higher-Order Theory for Laminated Composite Plates. *J. Appl. Mech.* **1984**, *51*, 745–752. [[CrossRef](#)]
19. Buitrago, B.L.; Santiuste, C.; Sanchez-Saez, S. Modelling of composite sandwich structures with honeycomb core subjected to high-velocity impact. *Compos. Struct.* **2010**, *92*, 2090–2096. [[CrossRef](#)]
20. Christiansen, E.L. Design and performance equations for advanced meteoroid and debris shields. *Int. J. Impact Eng.* **1993**, *14*, 145–156. [[CrossRef](#)]
21. Christiansen, E.L.; Kerr, J.H. Ballistic limit equations for spacecraft shielding. *Int. J. Impact Eng.* **2001**, *26*, 93–104. [[CrossRef](#)]
22. Sibeaud, J.M.; Thamie, L.; Puillet, C. Hypervelocity impact on honeycomb target structures: Experiments and modeling. *Int. J. Impact Eng.* **2008**, *35*, 1799–1807. [[CrossRef](#)]
23. Gilioli, A.; Sbarufatti, C.; Manes, A. Compression after impact test (CAI) on NOMEX (TM) honeycomb sandwich panels with thin aluminum skins. *Compos. Part B Eng.* **2014**, *67*, 313–325. [[CrossRef](#)]
24. de Souza, F. Experimental dynamic analysis of composite sandwich beams with magnetorheological honeycomb core. *Eng. Struct.* **2018**, *176*, 231–242. [[CrossRef](#)]
25. Dutra, J.R.; Luiz, M.; Christoforo, A.L. Investigations on sustainable honeycomb sandwich panels containing eucalyptus sawdust, Piassava and cement particles. *Thin-Walled Struct.* **2019**, *143*, 106191.1–106191.11. [[CrossRef](#)]
26. Du, W.Z. Study on Low Velocity Impact and Residual Compressive Strength of Composite Honeycomb Sandwich Structures. Master's Thesis, Jiangnan University, Wuxi, China, 2021.
27. Lv, X.Y.; Liu, L.Q.; Zhao, S.Y. Impact Penetration Test and Failure Mechanism of Thin-facesheets Composite Honeycomb Sandwich Structure. *Sci. Technol. Eng.* **2021**, *21*, 8834–8840.
28. Zhang, Y.W.; Yan, L.L.; Zhang, C. Low-velocity impact response of tube-reinforced honeycomb sandwich structure. *Thin-Walled Struct.* **2021**, *158*, 107188. [[CrossRef](#)]
29. Yasui, Y. Dynamic axial crushing of multi-layer honeycomb panels and impact tensile behavior of the component members. *Int. J. Impact Eng.* **2000**, *24*, 659–671. [[CrossRef](#)]
30. Li, M.; Liu, R.Q.; Luo, C.J. Numerical and experimental analyses on series aluminum honeycomb structures under quasi-static load. *J. Vib. Shock.* **2013**, *9*, 58–64.

Disclaimer/Publisher's Note: The statements, opinions and data contained in all publications are solely those of the individual author(s) and contributor(s) and not of MDPI and/or the editor(s). MDPI and/or the editor(s) disclaim responsibility for any injury to people or property resulting from any ideas, methods, instructions or products referred to in the content.